Improvement of the Structural Integrity of Ceramic Parts

Improvement of the Structural Integrity of Ceramic Parts:

Techniques and Applications

By

Bogdan Vasyliv

Cambridge Scholars Publishing

Improvement of the Structural Integrity of Ceramic Parts:
Techniques and Applications

By Bogdan Vasyliv

This book first published 2020

Cambridge Scholars Publishing

Lady Stephenson Library, Newcastle upon Tyne, NE6 2PA, UK

British Library Cataloguing in Publication Data
A catalogue record for this book is available from the British Library

ISBN (10): 1-5275-5588-7
ISBN (13): 978-1-5275-5588-4

TABLE OF CONTENTS

PREFACE

> "Though it's far from obvious, we live in a ceramic world, just as people have for thousands of years."
>
> —Chris Woodford, a British science writer
> https://www.explainthatstuff.com/chris-woodford.html

Advanced ceramics are ones that have been engineered (mostly since the early 20th century) for highly specific applications. For example, tungsten carbides and silicon nitrides are designed for making exceptionally hard cutting tools. Most modern engineered ceramics are metal oxides, carbides, and nitrides, which means they're compounds made by combining atoms of a metal with oxygen, carbon, or nitrogen atoms. Not all high-tech ceramic materials are simple compounds. Some are composite materials, in which the ceramic forms a kind of background material called the matrix, which is reinforced with fibers of another material (often carbon fibers, or sometimes fibers of a totally different ceramic). A material like this is known as a ceramic matrix composite.

This book proposes new approaches for solving the problems of quality control of manufactured ceramic products. One of them is the improvement of the material test method for chevron notched specimens, namely the use of a notch with oblique front (unsymmetrical chevron notch) in a compact specimen of small size under wedge loading. The second approach relates to the substantiation of the energetic basis for the crack retardation in a particular profile. Analytical solutions are proposed for calculating the crack growth resistance characteristics in ceramic products of certain geometry and predicting their service life under the action of static and cyclic (fatigue) loads. Also, a technique of preparing small specimens from industrial ceramic components has been developed. For substantiation of the use of such small size specimens, the fatigue crack growth rate (da/dN) versus the stress intensity factor range (ΔK) diagrams (da/dN–ΔK curves) were constructed using data obtained on specimens of different shapes and sizes. Based on the diagrams certain ranges of specimen sizes providing invariant fatigue crack growth resistance characteristics were defined. Regularities of crack retardation kinetics versus its profile angle for various ceramic materials have been found, and a concept of variable length of the crack front has been developed for estimating the lifetime of ceramic parts of various shapes. This concept has been successfully checked on hard alloy teeth of industrial drill bits. Also, such a shape-dependent crack deceleration approach was used for the substantiation of the shape of a solid oxide fuel cell (SOFC) anode substrate in comparison with the classic stress-strain approach. Among the existing fuel cells, SOFCs prove to be most promising because even now they exhibit the highest economic characteristics. It is time to continue their commercial production and the main attention of researchers should be focused on the optimization of the design of cells produced from layered macrocomposites and the investigation of the degradation of properties of these important power-generating units. The YSZ–NiO and ScCeSZ–NiO ceramics prove to be promising materials for the anode substrates of the SOFC. However, in certain stages of operation of the SOFC, the material of the anode may suffer the actions of high-temperature reducing-and-oxidizing (redox) gaseous atmospheres, as a result of random penetration of air into the fuel channels. The influence of the oxidation and corresponding reduction cycles is, as a rule, regarded as negative and undesired. In this work, the influence of high-temperature reducing and oxidizing gaseous atmospheres, as well as their repeated actions, is considered in the context of structural changes followed by corresponding changes in physicomechanical characteristics. It is revealed that at certain modes of heating and holding in reducing and oxidizing atmospheres, improvements of the structural integrity and functional characteristics of Ni-containing anode substrates for a SOFC can be reached. Based on such positive changes, the cyclic redox treatment technique is developed. The advantages of the application of such treatment for preconditioning of Ni-containing anode substrates are discussed.

The modes of cyclic redox treatment stages for the anode materials were substantiated on the base of mechanical and physical tests, studies of microstructure and fracture surface morphology using SEM (scanning electron microscopy) and an energy-dispersive X-ray microanalysis.

The work was carried out at Karpenko Physico-Mechanical Institute in Lviv, Ukraine. I would like to express my gratitude to my colleagues, first of all to Dr. Viktoriya Podhurska, as well as Dr. Andrii Ivasyshyn for providing an excellent working environment both scientifically, technically and on a personal level; also the late Dr. Andrii Bassarab for the inspirational support when starting the research. Special thanks to Prof. Orest Ostash for the critical analysis of the approaches presented in this book. Also a word of appraisal for colleagues at Frantsevich Institute for Problems of Materials Science (Kyiv, Ukraine), to Prof. Oleksandr Vasylyev for engaging in this cooperation, to Dr. Yehor Brodnikovskyi for preparing the anode materials

on which a significant part of the results was obtained. Without their commitment, this work would not have had the present quality or consistency.

Bogdan Vasyliv

INTRODUCTION

Among the methods of quality control of manufactured ceramic products, an important place belongs to the methods of fracture mechanics using specimens of the material. However, in many cases, when the size of the products is much smaller than the size of the standard test specimens for determination of the crack growth resistance characteristics, more flexible approaches are needed in the application of fracture mechanics. This requires the adaptation of the loading schemes and configuration of the specimens to obtain invariant data that can be used as indicators of the mechanical stability of the material and to predict the lifetime of the product of a particular configuration.

This book proposes new approaches to solving such problems. It consists of three parts.

The first part presents developed techniques of crack initiation and retardation in ceramics. In the beginning, a review of the historical development of chevron-notched fracture specimens has been performed. Stress intensity factors and load line displacement solutions proposed for some of these specimens are also compared. The review covers the original bend-bar configurations up to the present day "short" rod and bar specimens. The chevron-notched rod, bar, and bend-bar specimens were developed to determine the fracture toughness of brittle materials, materials that exhibit "flat" or "nearly flat" crack-growth resistance curves.

A procedure of crack initiation in a ceramic specimen at the tip of a notch with the oblique front has been developed. Based on this method, the conditions of the stable initiation and growth of cracks in specimens of brittle tool materials prepared for static and cyclic tests have been experimentally determined. The developed procedure of crack initiation in specimens from notches with the oblique front is applicable for brittle materials (ceramics, cermets, superhard materials) to determine the characteristics of crack resistance of these materials in the process of subsequent growth of these cracks under monotonic or cyclic loading.

The energetic conditions of stable crack initiation and growth from the tip of a notch with the oblique front in specimens made of brittle tool-making materials are substantiated using experimental data on the crack running and stopping moments, as functions of the crack length. A dynamic fracture resistance parameter called the specific fracture energy flux can be defined as an integral of the applied moment over time, per unit increment of the surface area of the crack. It can be used to characterize crack acceleration (or deceleration) in industrial parts of various profiles, made of brittle materials. The specific fracture energy flux is a parameter that exhibits the resistance of a material to crack growth in a product of a certain geometric profile. It is found that a crack in the product made of a brittle tool material decelerates if the crack front length increases more steeply than the flux of external energy.

A technique of preparing small C(T) [or DC(T)] specimens from industrial ceramic components, with the overall dimensions according to ASTM E 647, has been proposed. A crack in such a specimen is initiated at the tip of an unsymmetrical chevron (oblique) notch. The specimen is loaded monotonically by wedging in a direction perpendicular to the cutout plane. Since a load of crack nucleation is low, the elastic stored energy in the test specimen and testing apparatus is small. So the initiated crack then grows steadily, in particular, because of its profile. After initiating the crack in the manner described above, one can advance the crack under monotonic or cyclic loading to achieve its length close to that in a C(T) or DC(T) specimen. Then the holes (or a slot for a knife-edge loading fixture) for the eccentric tension of the specimen and a straight-through notch along the crack plane are made by electrical-discharge machining. As a result, a C(T) or DC(T) specimen is obtained with a crack formed, in which the required ratios of geometric dimensions were obtained. The specified specimens, despite their small sizes, allow determining accurately the whole set of crack growth resistance characteristics of the material of a product, including in the operating or model environment.

The advantages of controlled initiation of a crack at the oblique notch tip and its stable growth in the profile of a compact specimen under wedge loading, compared to other methods, are substantiated. It is shown that the compact specimens made of brittle materials using the mentioned technique are valid for the cyclic crack growth resistance evaluation in the frames of linear fracture mechanics.

The fatigue crack growth rate diagrams (da/dN–ΔK curves) were constructed using data obtained on specimens of different shapes and sizes. Based on the diagrams, certain ranges of specimen sizes providing invariant fatigue crack growth resistance characteristics were defined.

A developed procedure of crack initiation and propagation in a ceramic specimen with an unsymmetrical chevron profile and corresponding formulae for compliance calibration have been used to estimate the dynamics of crack growth in ceramic parts of various shapes. Based on the obtained experimental data the conditions of crack acceleration, quasi-equilibrium crack growth, and its deceleration were estimated.

The second part presents the results of the applications of the developed techniques. A method for fatigue testing and rapid analysis of the resistance of the WC–Co hard alloy teeth of drill bits to cyclic deformation has been proposed. This method is based on the evaluation of their limited endurance according to the initial magnitude of the maximum compressive load in a loading cycle and degree of its lowering in response to cyclic bearing in the process of strain-controlled testing. The efficiency of the proposed procedure is illustrated by the investigation of teeth made of WC–6 wt% Co, WC–8 wt% Co, and WC–12 wt% Co hard alloys. By using the parameters proposed, one can perform the rapid analysis of the quality of industrial lots of teeth of the same geometry but with different structures and made of different alloys. The values of the indicated parameters characterize both the ultimate load that can be withstood by the teeth under certain conditions and their susceptibility to crushing of the working surface under cyclic loading. Moreover, based on the regulatory values of the parameters proposed, one can perform the process of rejection of defective products. Unfortunately, these parameters are not characteristics of the material. Therefore, to evaluate endurance by using the proposed method, it is necessary first to accumulate a sufficiently large amount of data about different types of teeth, which can then be used to establish the relevant standard specifications and for the evaluation of the quality of teeth in the stage of manufacturing.

The damage kinetics in the material of the WC–Co hard alloy teeth under cyclic compressive loading is investigated. Three stages of damage to the microstructure up to the final fracture of a tooth are found. The dependences of the relative duration of each stage on the amplitude of the applied loading and the alloy composition are established. These dependences can be reconstructed so that they allow one, for a certain loading level and material of the tool, to establish directly the relationship between the degree of damage to the operating tool and its residual service life.

A developed procedure of crack initiation and propagation in a ceramic specimen profile with increasing crack front length and corresponding formulae for compliance calibration are used to estimate the dynamics of crack growth in hard alloy teeth of drill bits. For the specimens of an arbitrary shape made of brittle tool-making materials, the energetic conditions of stable crack initiation and growth can be substantiated using experimental data on the crack running and stopping moments, as functions of the crack length. Based on the obtained experimental data the conditions of crack acceleration, quasi-equilibrium crack growth, and its deceleration are estimated.

To contribute to reducing drilling costs, a specialized focus on drill bits and the factors affecting their performance should be provided. While the bit itself represents a small portion of the total drilling cost, its performance depends on correct utilization taking into account the rig capability, bottom hole assembly, mud, and the formation to be drilled. It is known that in many cases WC–Co hard alloy inserts of drill bits fail following long-term action of both the external loading and service environment. A microcrack set develops after the initial plastic deformation of the hard alloy tooth under operating conditions before material crumbles out and final failure occurs. A careful examination of the cyclic tooth-to-tooth compression test data reveals that a critical crack size, before tooth final failure, is about 0.8–1.5 mm. This fact requires evaluation of resistance to fatigue crack propagation in the material, which is characterized by the parameters such as fatigue crack growth rate, da/dN, and stress intensity factor (SIF) range, ΔK. Hence, to predict the lifetime of the hard alloy tooth a parameter which indicates the number of loading cycles to reach a crack increment of 1 mm is proposed. This parameter, $N_{\Delta K} = 1/(da/dN)$, is estimated using $da/dN - \Delta K$ curves of material at the certain ΔK value. To investigate fatigue crack growth behavior of brittle materials the promising test method based on small samples cut of industrial parts has been used. The crack growth kinetics in the WC–Co hard alloys under cyclic sine loading and constant long-term loading are investigated at room temperature in air and fluids with pH 4.5, 7, and 10.5. A significant difference in fatigue crack growth rates at low stress-intensity factor ranges is substantiated using the data of the polarization tests of the material in fluids with pH from 0.3 to 12.8. It is revealed that selective anodic dissolution of the cobalt phase and its embrittlement by hydrogen (the corrosion and hydrogen damage mechanisms respectively) accompanying cyclic loading of the WC–Co hard alloys in these fluids lead to a significant drop of fatigue crack growth resistance. The influence of chemical composition as well as material stress state and durability of environmental action on the corrosion-fatigue damage to the hard alloy under cyclic sine loading and constant long-term loading is evaluated. It is revealed that the lower lifetime of hard alloy inserts of drill bits in a service environment corresponds to hydrogen embrittlement of the cobalt phase.

In this part, the improved shape of an anode substrate for a solid oxide fuel cell (SOFC) has been suggested. The anode shape is substantiated using both the classic stress-strain and developed shape-dependent crack deceleration approaches. Stress and strain distributions in a YSZ–NiO spheroidal shape anode under pressure of the operating environment are calculated using the finite element analysis. The features are compared with ones of the cylindrical shape anode. Based on the calculations, dimensions and their ratios ranges are defined which correspond to improved stress-strain characteristics of the anode. According to this, an anode of the cylindrical shape with top and bottom convex surfaces (a spheroidal shape anode), with the spheroid to cylinder radii ratio R/R_c in the range from 5 to 20 is suggested. Its specific volume V/S_c (related to the base area S_c of its cylindrical part) is in the range from 1 to 2.5 mm. The stresses in the most dangerous areas (i. e. along the axis and the closed-loop fixing) and maximum strain, caused by external gas pressure on the anode working surface, are decreased by 10–30% and 20–40% respectively as compared to an anode of the cylindrical shape of the same radius and volume features. This increases the lifetime of a SOFC. A three-dimensional curve of intersection of the surfaces of stress distribution in the anode along its axis and the closed-loop fixing was approximated which displays the values of balanced stresses depending on V/V_c and R/R_c parameters. The advantage of the spheroid shaped SOFC anode substrate over conventional flat one was substantiated using a shape-dependent crack deceleration approach. It was concluded that in the case of a spheroidal shape anode, crack retardation occurs when the current value of the crack profile angle is about 10 degrees or more.

The third part presents a developed technique of the redox treatment of Ni-containing SOFC anodes and its application. A procedure and instruments have been developed for the strength analysis of ceramic disk specimens under the conditions of biaxial bending according to the ring–ring scheme at high temperatures (up to 800°C) in an operating hydrogen-containing medium of a solid oxide fuel cell with continuous measuring of the physical characteristics of materials (electrical resistivity or conductivity) as functions of time. The proposed procedure includes two consecutive steps, namely, the preliminary step of heating of the specimen from room temperature to a temperature of 600°C (or more) in air or an inert gas atmosphere, and the step of the gas evacuation from the chamber followed by the inlet of a hydrogen-containing gaseous mixture or purified hydrogen. The time dependences of the conductivity and strength characteristics of the anode ceramics with various contents of NiO obtained by using the proposed procedure can be used for the optimization of their chemical compositions.

A procedure of cyclic thermal treatment of ScCeSZ–NiO ceramics each separate cycle of which includes the reduction of the material in highpurity hydrogen (99.99 vol% under a partial pressure of 0.12 MPa) for 4 h at 600°C with subsequent oxidation in air (without a partial pressure) under the same conditions, is proposed. This enables us to obtain a material with satisfactory electrical conductivity after the third cycle of treatment, despite the lowered content of nickel oxide. It is reasonable to form the structure of the ceramic anode substrate by heating it to a temperature of 600°C in vacuum or an inert atmosphere and reducing the already heated material in hydrogen to prevent the phase transformations and formation of microcracks in the anode material in the course of heating. The procedure of oxidation of metallic nickel (formed in ScCeSZ–NiO ceramics as a result of the nickel oxide reduction in hydrogen) in air at 600°C prevents its coagulation. After three redox cycles carried out at 600°C, a network of fine (0.5–1.5 μm) particles of metallic nickel, uniformly distributed in the structure of the ceramic matrix is formed. As a result, the stabilization of the electrical conductivity of the fuel cell anode material is attained, and in the case of low contents of nickel oxide, the satisfactory electrical resistance of the material can be reached with preserving the level of strength typical of the as-sintered state.

It is revealed the positive effect of cyclic redox treatment at 600°C on the strength and electrical conductivity of anode substrates for SOFCs. As a result of this treatment of ceramic anodes of the 10Sc1CeSZ–50NiO and 8YSZ–50NiO systems, which includes the stages of heating up to a fixed temperature (600°C) in vacuum or an inert atmosphere, reduction of the preheated material in hydrogen-containing atmospheres, degassing, and oxidation in air at the same temperature, structures are formed guaranteeing the improved physicomechanical properties (strength and electrical conductivity) of these products.

The role of structural transformations in the nickel phase under the action of reducing and oxidizing high-temperature (600°C) gaseous atmospheres in the formation of the levels of strength and electrical conductivity of NiO-containing materials for the anodes-substrates of SOFCs is studied. By using the cyclic redox treatment of nickel oxide, we managed to form a structure guaranteeing the improved physicomechanical characteristics of YSZ–Ni and ScCeSZ–Ni composites.

The influence of redox cycling at the treatment temperatures of 600 and 800°C on the structure, strength and electrical conductivity of the YSZ–NiO ceramic anode substrates for SOFCs is analyzed. Based on the experimental data, we suppose that redox cycling at 600°C is the most ideal for this material. The parameters of the treatment (reduction holding time not less than 4 h under the pressure of Ar–5 vol% H_2 mixture of 0.15

MPa; oxidation holding time 4 h) allow a structure to be formed which provides improved physical and mechanical properties of the material. In such a structure, according to the X-ray analysis, a substantial drop of residual stresses is achieved as compared to the one-time reduced material. In contrast to this, at the treatment temperature 800°C, an anode structure with an array of microcracks is formed that significantly reduces the strength and electrical conductivity of the material.

Some reasons for nickel-zirconia SOFC anodes structural degradation in operating media are explained. The dual effect of water vapor on the YSZ–NiO ceramic anode durability is revealed. A small amount of water vapor in Ar–5 vol% H_2 mixture (water vapor pressure below 0.03 MPa) did not affect the reduction of the nickel phase in YSZ–NiO ceramics but caused some changes in the YSZ–Ni cermet structure, in particular, growth of nanopores in tiny Ni particles. The resulting strength of the YSZ–Ni cermet decreased by 10–12% as compared to the material reduced in the atmosphere without water vapor. A high concentration of water vapor in the mixture (water vapor pressure above 0.03–0.05 MPa) caused a converse change in the kinetics of reduction. The water vapor was an obstacle for the as-sintered material reduction and also caused re-oxidation of the nickel phase in the YSZ–Ni cermet at 600°C. Better physical and mechanical properties were revealed for material treated by redox cycling after holding at 600°C in the water-depleted gas mixture. Thus, the water vapor content in operating hydrogenous media of SOFCs has to be limited, and water vapor pressure should be below 0.03–0.05 MPa.

The substructure changes in the YSZ–NiO ceramic material for SOFC anodes, during its reduction and oxidation at 600°C, are studied. A series of the YSZ–NiO specimens were undergone to three treatment modes at 600°C, namely: (1) one-time reduction in a hydrogenous atmosphere; (2) redox cycling (five cycles), each redox cycle comprises the stages of isothermal holding in a hydrogenous atmosphere and air; and (3) redox cycling (five cycles), with extra stages of degassing. Two extra modes were used to simulate the behavior of materials in a water vapor containing atmosphere. Increased porosity, along with an increased amount of reduced Ni, has been revealed in specimens after mode 2 test. It was established that in the case of such treatment, a reaction of oxygen with the remaining hydrogen in the stage of isothermal holding in air at 600°C takes place followed by a substantial increase of water vapor local pressure. Such high-pressure conditions occur in small pores causing nucleation of nanocracks on three-phase ("nickel phase-zirconium phase-pore") boundaries. Such an effect of water vapor is probably the main reason for the structural degradation of the cermet. After mode 3 test of specimens, it was revealed that the stage of degassing between half-cycles of reduction and oxidation plays a substantial role in the formation of a Ni-network. Contrary to mode 2, the following structural peculiarities were detected: (1) formation of a network of nanopores in the particle outer layer; (2) reduction of the Ni-phase particle size by separating thin pieces of reduced Ni subgrains; (3) redistribution of fine Ni particles that allows the porosity to be partially decreased; and (4) formation of a network of reduced Ni particles that improves electrical conductivity and structural strength of the cermet. All these changes allow improving the electrical conductivity and structural strength of the cermet. The developed treatment technique promises to enhance the operational efficiency of SOFCs.

The influence of hydrogen sulfide amount in a hydrogenous atmosphere on the structure, physical, and mechanical properties of SOFC anode materials is studied. A series of specimens of porous nickel, YSZ–Ni cermet, and Ni–Al composite are investigated. To obtain the corresponding YSZ–Ni cermet structure, specimens of the YSZ–NiO ceramics were singly reduced in a hydrogenous atmosphere. A part of the specimens was then aged in a hydrogen sulfide containing atmosphere (7 or 18 vol% H_2S depending on a test mode). It is found that the relative strength and stiffness of porous Ni decrease with increasing hydrogen concentration. Neither 7 nor 18 vol% H_2S in a hydrogenous atmosphere affects plasticity, strength, and electrical conductivity of the material. It is revealed that the atmosphere containing up to 7 vol% H_2S has a slight effect on the strength and electrical conductivity of the YSZ–Ni cermet. Increased content of H_2S (18 vol%) causes some changes in the YSZ–Ni cermet structure. Multiple breaking of the zirconia-nickel bonds occurs that results in reduced strength of the cermet (by 39% as compared to as-received ceramics). It is revealed that the Ni–Al composite is not sensitive to a high-temperature hydrogenous atmosphere containing up to 7 vol% H_2S, which is reflected in stable values of strength, stiffness, and electrical conductivity. Thus, this composite is a promising material for manufacturing novel SOFC anodes resistible against hydrogen sulfide assisted structural degradation.

The work was carried out at Karpenko Physico-Mechanical Institute in Lviv, Ukraine. A significant part of the results was obtained on the SOFC anode materials prepared by researchers of Frantsevich Institute for Problems of Materials Science (Kyiv, Ukraine).

PART 1:

TECHNIQUES OF CRACK INITIATION AND RETARDATION IN CERAMICS

CHAPTER 1.1.

THE HISTORICAL DEVELOPMENT OF CHEVRON-NOTCHED SPECIMENS: A REVIEW

Summary. This chapter reviews the historical development of chevron-notched fracture specimens; it also compares stress intensity factors and load line displacement solutions that have been proposed for some of these specimens. The review covers the original bend-bar configurations up to the present day "short" rod and bar specimens. The chevron-notched rod, bar, and bend-bar specimens were developed to determine fracture toughness of brittle materials, materials that exhibit "flat" or "nearly flat" crack-growth resistance curves.

Nomenclature

A	normalized stress intensity factor defined by Barker
a	crack length measured from either front face of bend bar or load line
a_0	initial crack length (distance from load line to tip of chevron notch)
a_1	crack length measured to where chevron notch intersects specimen surface
a_m	crack length at which Y^* is minimum
b	length of crack front
B, D	thickness of bar specimen or diameter of rod specimen
C	specimen compliance, $C = EBV/P$
C^*	normalized compliance, $EBVL/P$, for chevron-notched specimen
C'	compliance derivative, $dC/d\alpha$
E	elastic (Young's) modulus
F	normalized stress intensity factor for straight-through crack specimen
F^*	normalized stress intensity factor for chevron-notched specimen

F^*_c	normalized stress intensity factor determined from compliance for chevron-notched specimen
F^*_m	minimum normalized stress intensity factor for chevron-notched specimen
H	half of bar specimen height or radius of rod specimen
K, K_I	opening-mode stress intensity factor (Mode I)
K_m	minimum stress intensity factor for chevron-notched specimen
K_{Ic}	plane-strain fracture toughness (ASTM E399)
K_{Icv}, K_{Iv}	plane-strain fracture toughness for chevron-notched specimen
K_R	crack-growth resistance
k	shear-correction parameter in Bluhm's slice model
P	applied load
P_{max}	maximum test (failure) load
V	crack mouth opening displacement
V_L	load-point half-displacement
V_T	half-displacement measured at top of specimen along load line
W	specimen width
x,y,z	Cartesian coordinates
Y^*	dimensionless stress intensity factor for a crack in a chevron notch, $K_I B W^{1/2}/P$
Y^*_m	minimum value of Y^* as a function of α
α	crack length-to-width (a/W) ratio
α_i	crack length-to-width (a_i/W) ratios defined in Fig. 1.2
α_0	initial crack length-to-width (a_0/W) ratio
α_m	crack length-to-width (a_m/W) ratio at which Y^* is minimum
ν	Poisson's ratio

History of chevron-notched specimens

Chevron-notched specimens (Fig. 1.1.1) are gaining widespread use for fracture toughness testing of ceramics, rocks, high-strength metals, and other brittle materials [1–8]. They are small (5- to 25-mm thick), simple, and inexpensive specimens for determining the plane-strain fracture toughness, denoted herein as K_{Icv}. Because they require no fatigue precracking, they are also well suited as quality control specimens.

The unique features of a chevron-notched specimen, over conventional fracture toughness specimens, are: (1) the extremely high stress concentration at the tip of the chevron notch, and (2) the stress intensity factor passes through a minimum as the crack grows. Because of the high-stress concentration factor at the tip of the chevron notch, a crack initiates at a low applied load, so costly precracking of the specimen is not needed. From the minimum stress intensity factor, the fracture toughness can be evaluated from the maximum test load. Therefore, a load-displacement record, as is currently required in the ASTM E399 plane-strain fracture toughness (K_{Ic}) test procedure, is not needed.

In 1964, Nakayama [2, 3] was the first to use a bend specimen with an unsymmetrical chevron notch. His specimen configuration is shown in Fig. 1.1.1a. He used it to measure fracture energy of brittle, polycrystalline, refractory materials. All previous methods which had been developed for testing homogeneous materials were thought to be inadequate. This specimen is unique in that a crack initiates at the tip of the chevron notch at a low load, then propagates stably until catastrophic fracture. Because of the low load, the elastic stored energy in the test specimen and testing apparatus was small so that the fracture energy could be estimated from the area under a load-time history record.

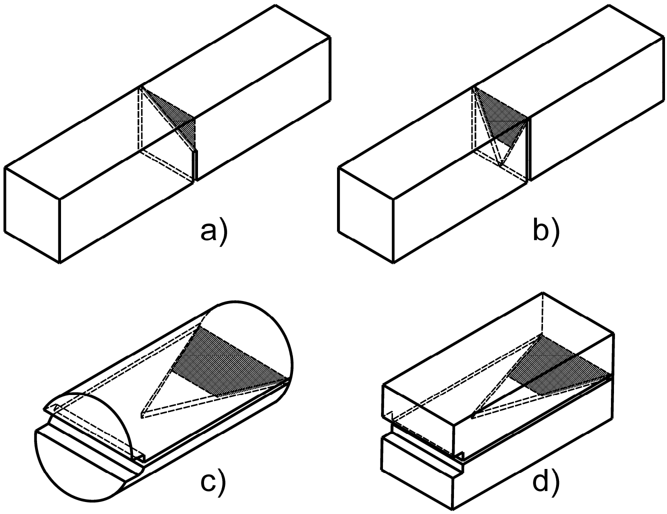

Fig. 1.1.1. *Various chevron-notched fracture specimen configurations: (a) a bend bar with an unsymmetrical chevron notch (Nakayama, 1964); (b) a bend bar with a chevron notch symmetrical about the center line of the specimen (Tattersall and Tappin, 1966); the knife-edge loaded (c) "short" rod (Barker, 1977) and (d) bar (Barker, 1978) chevron-notched specimens.*

Tattersall and Tappin [4] in 1966 proposed using a bend bar with a chevron notch symmetrical about the center line of the specimen, as shown in Fig. 1.1.1b. They used this specimen to measure the work of fracture on ceramics, metals and other materials. The work of fracture was determined from the area under the load-displacement record divided by the area of the fracture surfaces.

In 1972, Pook [5] suggested using a chevron-notched bend bar to determine the plane-strain fracture toughness of metals. He stated that, "If the K_I against crack length characteristic is modified, by the introduction of suitably profiled side grooves, so that there is a minimum at $a/W \sim 0.5$, and the initial K_I is at least twice this minimum, it should be possible to omit the precracking stage, and obtain a reasonable estimate of K_{Ic} from the maximum load in a rising load test". Pook's "suitably profiled side grooves" is the present day chevron notch. However, he considered only the analytical treatment needed to obtain stress intensity factors as a function of crack length for various types of chevron notches. He did not study the experimental aspects of using a chevron-notched specimen to obtain K_{Ic}.

The nomenclature currently used for a straight-sided chevron notch in a rectangular cross section specimen is shown in Fig. 1.1.2.

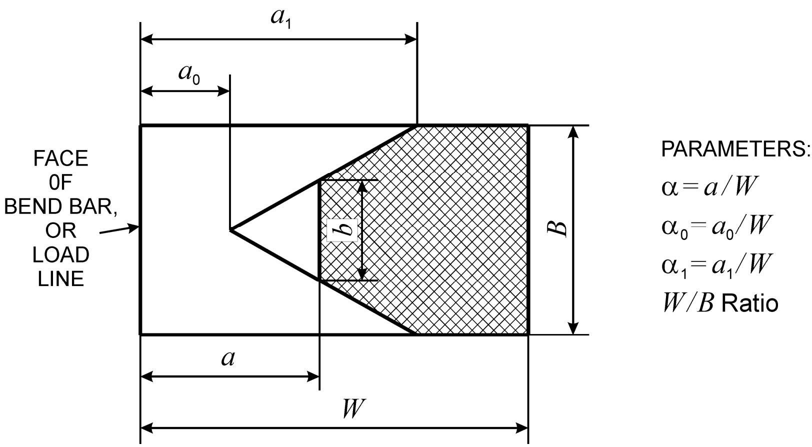

Fig. 1.1.2. *Chevron-notched fracture specimen nomenclature.*

The specimen width, W, and crack length, a, are measured from the front face of the bend bar (or from the load line in the knife-edge-loaded specimen). The dimensions a_0 and a_1 are measured from the edge of the bend bar (or load line) to the vertex of the chevron and to where the chevron intersects the specimen surface, respectively. The specimen is of thickness B and the crack front is of length b.

Pook [5] used the stress intensity factor solution for a three-point bend bar with a straight-through crack [9] and a side-groove correction proposed by Freed and Kraft [10] to obtain approximate solutions for various shape chevron notches. The stress intensity factor for a chevron-notched specimen, K_{CN} was given by

$$K_{CN} = K_{STC}\left(\frac{B}{b}\right)^{1/2} \tag{1.1.1}$$

where K_{STC} is the stress intensity factor for a straight-through crack in a bar having the same overall dimensions. The unique stress intensity factor solution for a chevron-notched specimen compared to a straight-through crack specimen is illustrated in Fig. 1.1.3.

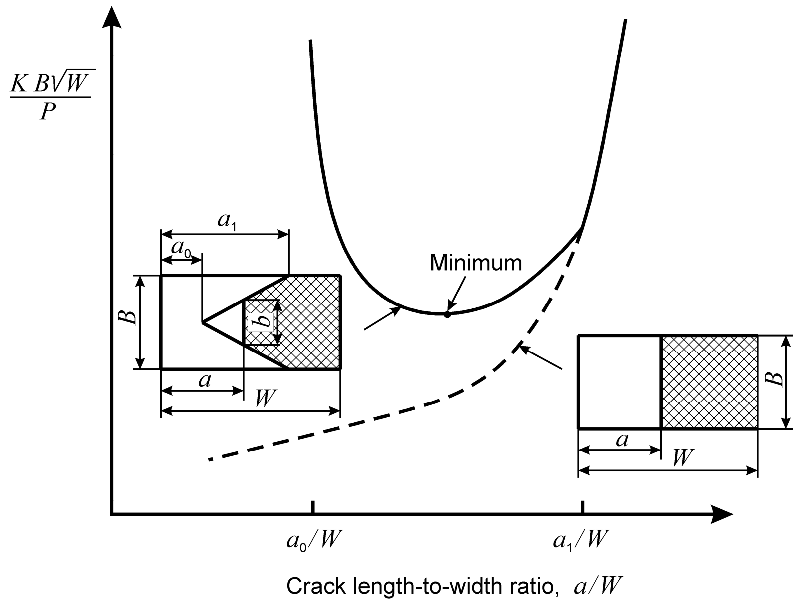

Fig. 1.1.3. *Comparison of normalized stress intensity factors for chevron-notched and straight-through crack specimens.*

The dashed curve shows the normalized stress intensity factors for the straight-through crack as a function of *a/W*. This curve is a monotonically increasing function with crack length.

The solid curve shows the solution for the chevron-notched specimen. For $a = a_0$, the stress intensity factor is very large but it rapidly drops as the crack length increases. A minimum value is reached when the crack length is between a_0 and a_1. For $a > a_1$, the stress intensity factors for the chevron-notched specimen and for the straight-through crack specimen are identical because the configurations are identical.

The analytical procedure used by Pook [5] to determine the stress intensity factor as a function of crack length was an engineering approximation. At that time, no rigorous analysis had been conducted to verify the accuracy of Eqn (1.1.1).

In 1975, Bluhm [11] made the first serious attempt to analyze the chevron-notched bend bars. The three-dimensional crack configuration was analyzed in an approximate "two-dimensional" fashion. The specimen was treated as a series of slices in the spanwise direction. Both beam bending and beam shear effects on the compliance of each slice were considered but the inter-slice shear stresses were neglected in the analysis. Then by a synthesis of the slice behavior, the total specimen compliance was determined.

The slice model, however, introduced a "shear correction" parameter (k) which had to be evaluated from experimental compliance measurements. Experimental compliance measurements made on an "uncracked" chevron-notched bend bar (α_0 =0 and α_1 = 1) were used to determine a value for the "shear correction" parameter for three- and four-point bend specimens. Bluhm estimated that the slice model was capable of predicting the compliance of the cracked Tattersall-Tappin type specimen (see Fig. 1.1.1b) to within 3 percent.

Bluhm did not, however, calculate stress intensity factors from the compliance equations. Later, Munz et al. [8] did use Bluhm's slice model to calculate stress intensity factors for various chevron-notch bar specimens.

The concept proposed by Pook [5] to determine the K_{Ic} value for brittle materials using chevron-notched specimens can be illustrated on the graph showing stress intensity factor, K, versus crack length (Fig. 1.1.4).

The solid line beginning at a_0 and leveling off at K_{Ic} is the "ideal" crack-growth resistance curve for a brittle material. The dashed curves show the "crack-driving force" curves for various values of applied load on a chevron-notched specimen. Because of the extremely large K value at $a = a_0$ a small value of load, like P_1 is enough to initiate a crack at the vertex of the chevron. At load P_1 the crack grows until the crack-drive value is equal to K_{Ic}, that is, the intersection point between the dashed curve and horizontal line at point A. Further increases in load are required to extend the crack to point *B* and *C*. When the maximum load, P_{max}, is reached the crack-drive curve is tangent to the K_{Ic} line at point *D*. Thus, the *K* value at failure is equal to K_{Ic}. The tangent point also corresponds to the minimum value of stress intensity factor on the crack-drive curve (denoted with a solid symbol).

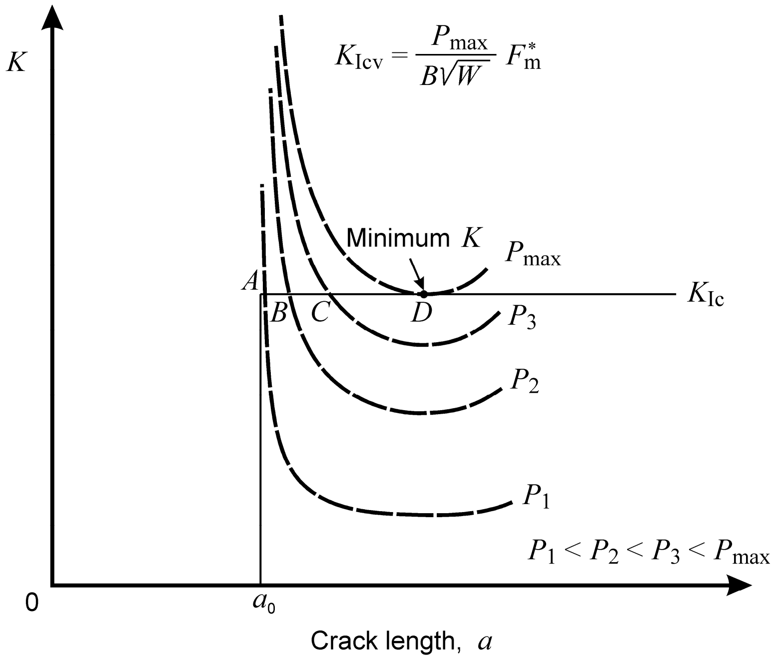

Fig. 1.1.4. *Fracture of "brittle" material using a chevron-notched specimen.*

Therefore, K_{Icv} is calculated by

$$K_{Icv} = \frac{P_{max}}{B\sqrt{W}} F^*_m \tag{1.1.2}$$

where P_{max} is the maximum failure load and F^*_m is the minimum value of the normalized stress intensity factor. Because F^* is a predetermined value for the particular chevron-notched configuration, it is necessary only to measure the maximum load to calculate K_{Icv}.

This maximum load test procedure can only be applied to brittle materials with flat or nearly flat crack-growth resistance curves. Many engineering materials, however, have a rising crack-growth resistance curve.

***

Although the bend bars were the first type of chevron-notched specimens to be tested, the knife-edge loaded rod and bar specimens have received more attention. Barker [6, 7] in the late 70's, proposed the "short" rod and bar specimens (Fig. 1.1.1c, d) for determining plane-strain fracture toughness. The coordinate system used to define dimensions of the most commonly used rod and bar specimens is shown in Fig. 1.1.5. These specimens are loaded by a knife-edge loading fixture [6, 8] resulting in an applied line load, P, at location L, as shown in Fig. 1.1.5a. (Here the chevron notch intersects the specimen surface at $x = W$ or $\alpha_1 = 1$.)

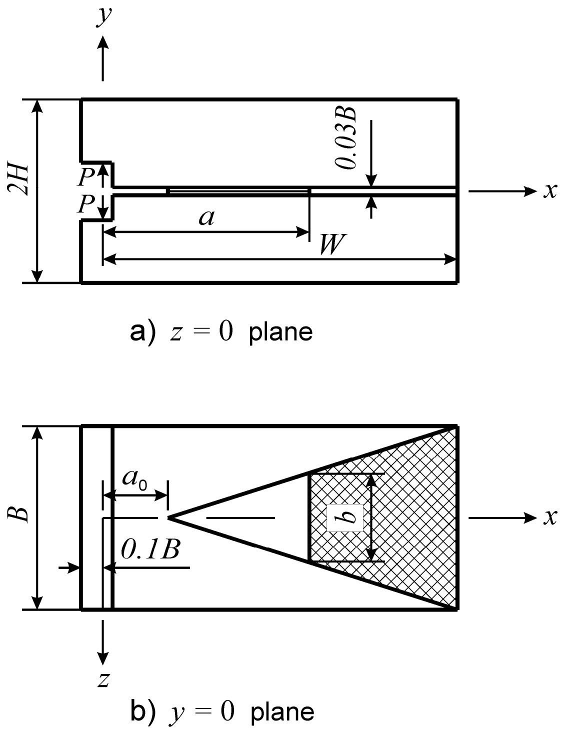

Fig. 1.1.5. *Coordinate system used to define dimensions of knife-edge loaded chevron-notched rod and bar specimens.*

Rod Specimens

Since 1977, the chevron-notched rod specimen, with W/B = 1.45, has been studied extensively (see Fig. 1.1.6a).

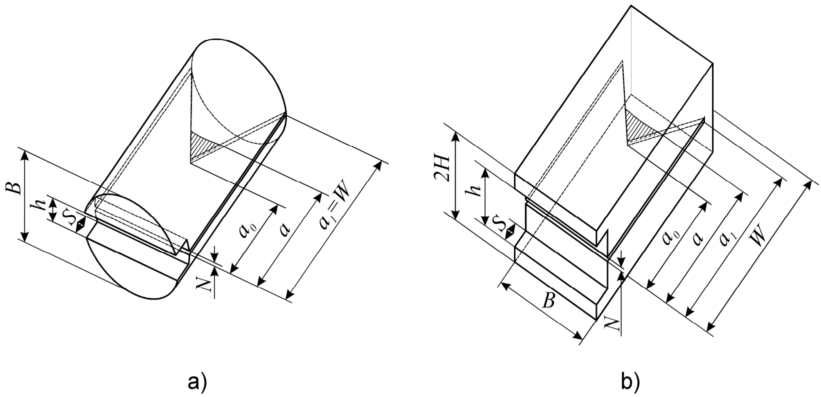

Fig. 1.1.6. *Chevron-notch (a) rod and (b) bar specimens*

In 1977, Barker [6] used the K_{Ic} value obtained from ASTM E399 compact specimens made of 2014-T651 aluminum alloy to determine the minimum stress intensity factor for the rod configuration by a "matching" procedure. The minimum stress intensity factor was given by

$$K_{m} = \frac{P_{max} A}{\sqrt{B^3(1-\nu^2)}} \tag{1.1.3}$$

where A is Barker's normalized stress intensity factor that accounts for the configuration. By equating K_m to K_{Ic}, the value of A was 20.8.

Eqn (1.1.3) can be rewritten into the form

$$K_{m} = \frac{P_{max}}{B\sqrt{W}} F_{m}^{*} \tag{1.1.4}$$

where the value of F^* is 26.3 (ν = 0.3). (Eqn (1.1.4) is the form commonly used for compact and knife-edge loaded specimens. The same form will be used herein.)

In 1979, Barker [12] replaced the term $(1-\nu^2)$ in equation (1.1.3) with unity without changing the value of A. Thus, the value of F^* dropped by about 5 percent. The value of F^*_m should have remained at 26.3 for ν = 0.3.

Barker and Baratta [13] in 1980 extensively evaluated the fracture toughness of several steel, aluminum, and titanium alloys using the rod specimen and K_{Ic} values measured according to ASTM Standard Method of Test for Plane strain Fracture Toughness of Metallic Materials (E399-78). They found that the critical stress intensity factors, calculated from the rod specimen data using F^*_m = 25.5 [13], were consistently low, averaging about 6 percent below the K_{Ic} values. They concluded that F^*_m for the test configuration used in their study should be increased by 4 percent to a value of 26.5.

Earlier, Barker and Guest [14] had conducted an experimental compliance calibration on the rod specimen and had obtained a value of F^*_m as 29.6. Their specimen, however, had a *W/B* ratio of 1.474 [15]. Subsequently, the value of F^*_m was corrected to a value corresponding to a *W/B* ratio of 1.45 by using a "constant moment" conversion described in reference [16].

Beech and Ingraffea [17, 18] were the first to rigorously numerically analyze a chevron-notched specimen. They used a three-dimensional finite-element method to determine stress intensity factor distributions along the crack front and stress intensity factors from compliance for the chevron notched rod.

Bubsey et al. [19], Shannon et al. [20], and Barker [16] used the experimental compliance (plane stress) relation to evaluate stress intensity factors for the "short" rod specimen.

Raju and Newman [21], using a three-dimensional finite-element method, studied the effects of Poisson's ratio (ν) on stress intensity factors for the rod specimen (W/B = 1.45).

Raju and Newman [21] and Ingraffea et al. [22] determined the minimum stress intensity factors for the rod specimen (W/B = 1.45) using compliance calculations from three-dimensional finite-element analyses.

Ingraffea et al. [22] also used a boundary-element (boundary-integral) method to determine the minimum stress intensity factor from compliance.

Bar Specimens

Two types of chevron-notched bar specimens have been studied. In 1978, Barker [7, 16] proposed a rectangular cross-sectioned bar specimen with an *H/B* ratio of 0.435 (see Fig. 1.1.6b).

In 1980, Munz et al. [8] proposed a square cross-sectioned bar specimen (H/B = 0.5). They conducted a very extensive experimental compliance calibration on bar specimens with W/B = 1.5 and 2 for α_0 ranging from 0.2 to 0.5 and α_1 = 1). From these results, they obtained minimum values of stress intensity factors for each configuration considered. Using the assumption that the change of compliance with crack length in a chevron-notch specimen was the same as that for a straight-through crack specimen, they obtained an equation that was identical to Eqn (1.1.1) as

$$F^* = F\left(\frac{\alpha_1 - \alpha_0}{\alpha - \alpha_0}\right) = F\left(\frac{B}{b}\right)^{1/2} \tag{1.1.5}$$

for $\alpha_0 < \alpha < \alpha_1$. For specimens with an α_0 of about 0.2 and 0.35, the difference between experimental and analytical (Eqn (1.1.5)) minimum normalized stress intensity factors was less than 1 percent. For an α_0 value of about 0.5, the difference was 3 to 3.5 percent. They concluded that Eqn (1.1.5) should only be used to obtain minimum values because experimental and analytical values differed greatly at small crack length-to-width (α) ratios near α_0.

Shannon et al. [20] have developed minimum stress intensity factor expressions for chevron-notched bar (square) and rod specimens with α_1 = 1 and $\alpha_0 < 0.5$. These expressions were fitted to minimum stress intensity factors determined from experimental compliance measurements. For the square bar specimen, the W/B ratio was 1.5 or 2 and for the rod specimen, the W/B ratio was 1.5, 1.75 or 2. The use of chevron-notched specimens with materials that have a rising crack growth resistance curve may require stress intensity factors as a function of crack length instead of using only the minimum value. Shannon et al. [23] have developed polynomial expressions that give the stress intensity factors and load-line displacements as a function of crack length for square-bar and rod specimens (α_1 = 1). These expressions were obtained from experimental compliance measurements made for various W/B ratios. The W/B ratio for the square-bar specimen was, again, 1.5 or 2, and for the rod specimen was 1.5, 1.75, or 2. The expressions apply to α_0 between 0.2 and 0.4, and α varying from α_0 to 0.8.

***